

Production cross sections of ${}^3,4_{\Lambda}\text{H}$ bound states in ${}^3,4\text{He}(K^-, \pi^0)$ reactions at 1 GeV/c

Toru Harada^{1,2,*} and Yoshiharu Hirabayashi³

¹*Center for Physics and Mathematics,
Osaka Electro-Communication University,
Neyagawa, Osaka, 572-8530, Japan*

²*J-PARC Branch, KEK Theory Center,
Institute of Particle and Nuclear Studies,
High Energy Accelerator Research Organization (KEK),
203-1, Shirakata, Tokai, Ibaraki, 319-1106, Japan*

³*Information Initiative Center, Hokkaido University, Sapporo, 060-0811, Japan*

(Dated: August 18, 2021)

Abstract

We investigate theoretically productions of ${}^3,4_{\Lambda}\text{H}$ bound states in the exothermic (K^-, π^0) reactions on ${}^3,4\text{He}$ targets at $p_{K^-} = 1.0$ GeV/c in a distorted-wave impulse approximation with the optimal Fermi-averaging $K^-p \rightarrow \pi^0\Lambda$ t matrix. We calculate angular distributions of the laboratory differential cross sections $d\sigma/d\Omega_{\text{lab}}$ and the integrated cross sections σ_{lab} for a $J^P = 0^+$ ground state and a $J^P = 1^+$ excited state of ${}^4_{\Lambda}\text{H}$ at π^0 forward-direction angles of $\theta_{\text{lab}} = 0^\circ\text{--}20^\circ$, and those for a $J^P = 1/2^+$ ground state of ${}^3_{\Lambda}\text{H}$. The production of a $J^P = 3/2^+$ excited state of ${}^3_{\Lambda}\text{H}$ as a virtual state is also evaluated. The comparison in $d\sigma/d\Omega_{\text{lab}}$ and σ_{lab} between ${}^4_{\Lambda}\text{H}$ and ${}^3_{\Lambda}\text{H}$ provides examining the mechanism of the production and structure of ${}^3,4_{\Lambda}\text{H}$, as well as in the endothermic (π^-, K^0) reactions at $p_{\pi^-} = 1.05$ GeV/c. This investigation confirms the feasibility of lifetime measurements of ${}^3_{\Lambda}\text{H}$ at the J-PARC experiments.

PACS numbers: 21.80.+a, 24.10.Ht, 27.30.+t, 27.80.+w

Keywords: Hypernuclei, DWIA, Cross section

*Electronic address: harada@osakac.ac.jp

I. INTRODUCTION

Recently, experimental measurements of a ${}^3_{\Lambda}\text{H}$ lifetime are planned by (K^-, π^0) and (π^-, K^0) reactions on a ${}^3\text{He}$ target at J-PARC [1, 2] to solve the puzzle that the unexpected short lifetime of ${}^3_{\Lambda}\text{H}$ was measured in hypernuclear production by high-energy heavy-ion collisions [3, 4]. It seems that it is rather difficult to form a Λ bound state by the nuclear (K^-, π^0) and (π^-, K^0) reactions because the Λ hyperon is very weakly bound in ${}^3_{\Lambda}\text{H}$ with a $J^P = 1/2^+$ ground-state (g.s.) separation energy $B_{\Lambda} = 0.13 \pm 0.05$ MeV [5] with respect to the d - Λ threshold, whereas a recent measurement by the STAR Collaboration reports a value of 0.41 ± 0.12 MeV [6].

On the other hand, the production of a $J^P = 0^+$ ground state of ${}^4_{\Lambda}\text{He}$ in the ${}^4\text{He}(K^-, \pi^-)$ reaction is accomplished theoretically [7, 8] and experimentally [9, 10], where the Λ is bound with $B_{\Lambda} = 2.39 \pm 0.05$ MeV with respect to the ${}^3\text{He}$ - Λ threshold. In a previous paper [11], we reexamined the production cross section of the $0^+_{\text{g.s.}}$ state of ${}^4_{\Lambda}\text{He}$ in the ${}^4\text{He}(\pi, K)$ reaction at $p_{\pi^-} = 1.05$ GeV/ c , and discussed a benefit of the use of a s -shell target nucleus for Λ production of the $A = 4$ hypernucleus. To study the feasibility of the lifetime measurements of ${}^3_{\Lambda}\text{H}$ in the production followed by mesonic decay processes [1], thus, it is worth examining theoretically the Λ production of the $A = 3$ hypernucleus via the (\bar{K}, π) or (π, K) reaction.

It has been recently discussed [12] that there is a s -wave virtual state with $J^P = 3/2^+$, $L = 0$ near the d - Λ threshold in the $d + \Lambda$ system, which may correspond to a $J^P = 3/2^+$ excited state (exc) of ${}^3_{\Lambda}\text{H}$ that has not yet been observed experimentally. Thus the production of the $3/2^+_{\text{exc}}$ state of ${}^3_{\Lambda}\text{H}$ via the ${}^3\text{He}(K^-, \pi^0)$ reaction also needs to be examined from a theoretical point of view.

In this paper, we investigate theoretically the productions of the ${}^{3,4}_{\Lambda}\text{H}$ bound states in the exothermic (K^-, π^0) reactions on ${}^{3,4}\text{He}$ targets at $p_{K^-} = 1.0$ GeV/ c in a distorted-wave impulse approximation (DWIA) using the optimal Fermi-averaging $K^-p \rightarrow \Lambda\pi^0$ t matrix [13]. We demonstrate angular distributions of the laboratory differential cross sections for ${}^4_{\Lambda}\text{H}(J^P = 0^+, \text{g.s.})$, ${}^4_{\Lambda}\text{H}(J^P = 1^+, \text{exc})$, and ${}^3_{\Lambda}\text{H}(J^P = 1/2^+, \text{g.s.})$ bound states in the π^0 forward-direction angles of $\theta_{\text{lab}} = 0^\circ\text{--}20^\circ$, and the integrated cross sections for them. We also investigate the production of ${}^3_{\Lambda}\text{H}(J^P = 3/2^+, \text{exc})$ as a virtual state close to the d - Λ threshold. We discuss the effects of a weakly Λ binding, a meson distortion, and an in-medium elementary amplitude in the nuclear (K^-, π^0) reactions, as well as in

the endothermic (π^- , K^0) reaction [11]. To reduce uncertainties of several approximations and input parameters in our calculations, we attempt to examine the difference in the Λ production between ${}^4_\Lambda\text{H}$ and ${}^3_\Lambda\text{H}$.

II. CALCULATIONS

A. Distorted-wave impulse approximation

Let us consider a calculation procedure of the Λ hypernuclear production for the nuclear (K^- , π) reaction in the laboratory frame. We will present briefly the standard DWIA calculation [14–16] applying to the productions of the ${}^{3,4}_\Lambda\text{H}$ bound states in the reactions



The differential cross section for the Λ bound state with a spin-parity J_B^P at the π^0 forward-direction angle of θ_{lab} is written [11] by (in units $\hbar = c = 1$)

$$\begin{aligned} \left(\frac{d\sigma}{d\Omega}\right)_{\text{lab}, \theta_{\text{lab}}}^{J_B^P} &= \alpha \frac{1}{[J_A]} \sum_{m_A m_B} \left| \left\langle \Psi_B \left| \bar{f}_{\pi^0\Lambda} + i \bar{g}_{\pi^0\Lambda} \boldsymbol{\sigma} \cdot \hat{\mathbf{n}} \right. \right. \right. \\ &\quad \left. \left. \left. \times \chi_{\pi}^{(-)*} \left(\mathbf{p}_{\pi}, \frac{M_C}{M_B} \mathbf{r} \right) \chi_{K^-}^{(+)} \left(\mathbf{p}_{K^-}, \frac{M_C}{M_A} \mathbf{r} \right) \right| \Psi_A \right\rangle \right|^2, \end{aligned} \quad (2)$$

where $[J] = 2J + 1$, and Ψ_B and Ψ_A are wave functions of the hypernuclear final state and the initial state of the target nucleus, respectively. The kinematical factor α denotes the translation from a two-body K^- -nucleon laboratory system to a K^- -nucleus laboratory system [17]. $\hat{\mathbf{n}}$ is a unit vector perpendicular to the reaction plane. $\chi_{\pi}^{(-)}$ and $\chi_{K^-}^{(+)}$ are meson distorted waves for outgoing π^0 and incoming K^- , respectively. The factors of M_C/M_B and M_C/M_A arise from the recoil correction, where M_A , M_B and M_C are the masses of the target, the hypernucleus, and the core nucleus, respectively. The energy and momentum transfers to the final state are given by

$$\omega = E_{K^-} - E_{\pi}, \quad \mathbf{q} = \mathbf{p}_{K^-} - \mathbf{p}_{\pi}, \quad (3)$$

where $E_{K^-} = (\mathbf{p}_{K^-}^2 + m_{K^-}^2)^{1/2}$ and $E_{\pi} = (\mathbf{p}_{\pi}^2 + m_{\pi}^2)^{1/2}$ (\mathbf{p}_{K^-} and \mathbf{p}_{π}) are the laboratory energies (momenta) of K^- and π^0 in this nuclear reaction, respectively; m_{K^-} and m_{π} are

the masses of K^- and π^0 , respectively. $\bar{f}_{\pi^0\Lambda}$ and $\bar{g}_{\pi^0\Lambda}$ describe the non-spin-flip $\Delta S = 0$ and spin-flip $\Delta S = 1$ amplitudes for the in-medium $K^-p \rightarrow \pi^0\Lambda$ production, respectively, which take into account the Fermi motion of a struck nucleon in the nuclear target for the nuclear (K^- , π^0) reaction. The explicit forms of Eq. (1) are given by Appendix A.

The Fermi-averaging treatment may essentially affect the absolute values of the production cross sections even through ${}^3_\Lambda\text{H}$ [18]. Here we apply the optimal Fermi-averaging procedure [13] to $\bar{f}_{\pi^0\Lambda}$ and $\bar{g}_{\pi^0\Lambda}$ in the nuclear (K^- , π^0) reaction; the momentum distribution $\rho(p)$ of the struck nucleon in ${}^3\text{He}$ (${}^4\text{He}$) is assumed as a simple harmonic oscillator with a size parameter $b_N = 1.61$ (1.33) fm, leading to $\langle p^2 \rangle^{1/2} \simeq 150$ (182) MeV/ c in the nucleus [19]. We employ the elementary $\bar{K}N \rightarrow \pi\Lambda$ amplitude analyzed by Gopal, et al. [20].

The distorted waves of $\chi_\pi^{(-)}$ and $\chi_{K^-}^{(+)}$ are obtained in a computational procedure simplified with the help of the eikonal approximation [14, 15]. We choose $\alpha_{K^-} = \alpha_\pi = 0$, $\sigma_{K^-} = 45$ mb, and $\sigma_\pi = 32$ mb in charge independence, as eikonal distortion parameters for the ${}^{3,4}\text{He}$ targets. Although such distortions are seemed to be not so important in the light s -shell nuclear systems than in p -shell nuclear systems like ${}^{12}\text{C}$, it is necessary to verify their effects on the production cross sections in more quantitative calculations [11].

B. Effective number of nucleons for ${}^3,4_\Lambda\text{H}$ bound-state productions

Considering the non-spin-flip $\Delta S = 0$ production in the ${}^{3,4}\text{He}(K^-, \pi^0)$ reactions, we obtain the differential cross sections of Eq. (2) for the production of ${}^3,4_\Lambda\text{H}$, which are often written by the effective number technique [14, 15];

$$\left(\frac{d\sigma}{d\Omega}\right)_{\text{lab},\theta_{\text{lab}}}^{J_B^P} = \alpha \left\langle \frac{d\sigma}{d\Omega} \right\rangle_{\text{lab},\theta_{\text{lab}}}^{\text{elem}} Z_{\text{eff}}^{J_B^P}(\theta_{\text{lab}}), \quad (4)$$

where $\alpha \langle d\sigma/d\Omega \rangle_{\text{lab}}^{\text{elem}} = \alpha |\bar{f}_{\pi^0\Lambda}|^2$ is a differential cross section for the in-medium $K^-p \rightarrow \pi^0\Lambda$ $\Delta S = 0$ reaction, including the kinematical factor α . The effective number of nucleons $Z_{\text{eff}}^{J_B^P}$ for the production of the ${}^3,4_\Lambda\text{H}(J_B^P)$ bound state is reduced [11] as

$$Z_{\text{eff}}^{J_B^P}(\theta_{\text{lab}}) = C_{TS}^2 |F(q)|^2, \quad (5)$$

where C_{TS} is the isospin-spin (TS) spectroscopic amplitude between the Λ final state and the N initial state. The form factor $F(q)$ is written by

$$F(q) = \int_0^\infty dr r^2 \rho_{\text{tr}}(r) \tilde{j}_0\left(q; \frac{M_C}{M_D} r\right), \quad (6)$$

TABLE I: Calculated Λ separation energies B_Λ and root-mean-square distances $\langle r_\Lambda^2 \rangle^{1/2}$ between the core nucleus and Λ in ${}^3,4\text{H}$ with an isospin T and a spin J^P , in comparison with B_N and $\langle r_N^2 \rangle^{1/2}$ for a nucleon in ${}^3,4\text{He}$ targets.

	$A = 3$			$A = 4$		
	${}^3_\Lambda\text{H}_{\text{g.s.}}$	${}^3_\Lambda\text{H}_{\text{exc}}$	${}^3\text{He}$	${}^4_\Lambda\text{H}_{\text{g.s.}}$	${}^4_\Lambda\text{H}_{\text{exc}}$	${}^4\text{He}$
T	0	0	1/2	1/2	1/2	0
J^P	1/2 ⁺	3/2 ⁺	1/2 ⁺	0 ⁺	1 ⁺	0 ⁺
$B_{\Lambda(N)}$ (MeV)	0.13	unbound ^a	5.49	2.16	1.09	19.8
$\langle r_{\Lambda(N)}^2 \rangle^{1/2}$ (fm)	11.2	18.2 ^b	2.49	3.68	4.60	1.87
B_Λ^{exp} (MeV)	0.13 \pm 0.05 [5]			2.04 \pm 0.04 [5]	0.95 \pm 0.04 [22]	
	0.41 \pm 0.12 [6]			2.16 \pm 0.08 [23]	1.09 \pm 0.02 [10]	

^aThe pole of the S matrix as the virtual state is located at $E_{\Lambda d}^{(\text{pole})} = -0.089$ MeV on the unphysical sheet [-].

^bThe continuum-discretized wave function is used. See text in Sect. II C.

where $\tilde{j}_0(q; r)$ is a distorted wave for the meson distortion; M_C/M_B and M_C/M_A in Eq. (2) are replaced by M_C/M_D in the eikonal approximation, where an averaged mass $M_D \equiv (M_B + M_A)/2$, which may give a good estimation for the very light nuclear systems. Because the factor of M_C/M_D originates from the recoil correction, the *effective* momentum transfer is often defined by $q_{\text{eff}} \equiv (M_C/M_D)q \simeq [(A-1)/A]q$, which controls effectively the recoil effects on the production cross sections in the eikonal approximation [15, 16]. When the distortion effects are switched off ($\sigma_{K^-}, \sigma_\pi \rightarrow 0$), the production cross sections can be obtained in the plane-wave impulse approximation (PWIA), with replacing $\tilde{j}_0(q; r)$ by $j_0(qr)$ that is a spherical Bessel function with $L = 0$ [11].

The transition density $\rho_{\text{tr}}(r)$ in Eq. (6) is given by

$$\rho_{\text{tr}}(r) = \varphi_0^{(\Lambda)*}(r)\varphi_0^{(N)}(r), \quad (7)$$

where $\varphi_0^{(\Lambda)} = \langle \phi_0^{(C)} | \Psi_B \rangle$ is the relative wave function that is regarded as a spectroscopic amplitude for Λ in ${}^3,4\text{H}$ by using the wave function $\phi_0^{(C)}$ for the core nucleus [21], and $\varphi_0^{(N)} = \langle \phi_0^{(C)} | \Psi_A \rangle$ is the relative wave function for a nucleon (N) in ${}^3,4\text{He}$. In Table I, we

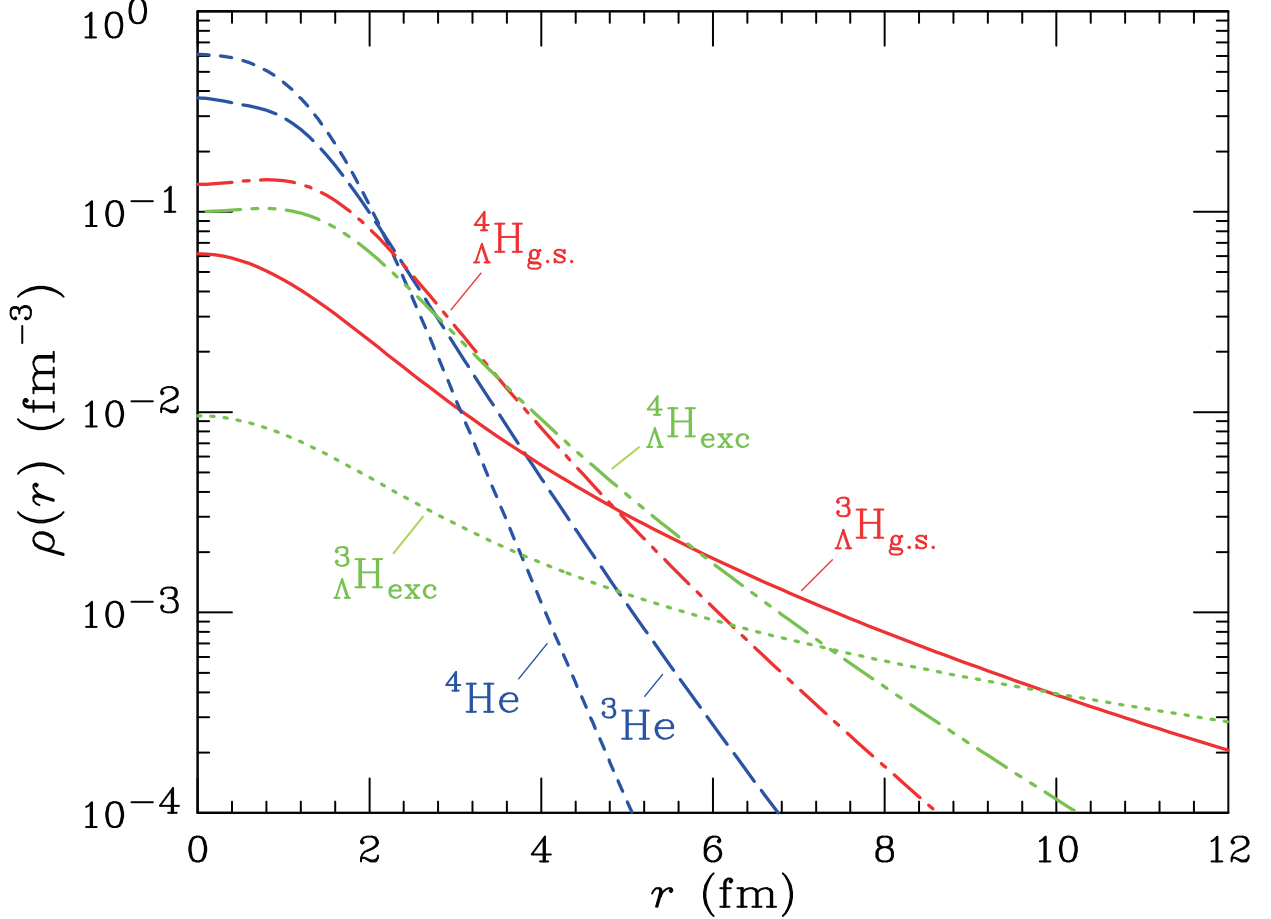


FIG. 1: Relative density distributions $\rho_\Lambda(r)$ for Λ in ${}^3,4_\Lambda\text{H}_{\text{g.s.}}$, as a function of the relative distance between the core nucleus and Λ , together with the relative density distributions $\rho_N(r)$ for a nucleon (N) in the ${}^3,4\text{He}$ targets. The relative density distributions for Λ in ${}^3,4_\Lambda\text{H}_{\text{exc}}$ are also drawn.

show the calculated Λ separation energies B_Λ and the root-mean-square distances $\langle r_\Lambda^2 \rangle^{1/2}$ between the core nucleus and Λ in ${}^3,4_\Lambda\text{H}$ with the isospin T_B and the spin J_B^P , together with the nucleon separation energies B_N and $\langle r_N^2 \rangle^{1/2}$ between the core nucleus and N in ${}^3,4\text{He}$ with T_A and J_A^P . For $A = 4$, we obtain $\varphi_0^{(\Lambda)}$ in the $3N$ - Λ model based on four-body $\Lambda N N N$ calculations [11] with central nucleon-nucleon (NN) and ΛN potentials, reproducing $B_\Lambda = 2.16$ MeV [23] and $\langle r_\Lambda^2 \rangle^{1/2} = 3.68$ fm for ${}^3\text{H} + \Lambda$ in ${}^4_\Lambda\text{H}$ ($J^P = 0^+$, g.s.). We use $\varphi_0^{(N)}$ obtained in four-body $N N N N$ calculations [21], and $C_{TS}^2 = 2$. For $A = 3$, we obtain $\varphi_0^{(\Lambda)}$ in the $2N$ - Λ model based on microscopic continuum-discretized coupled-channels (CDCC) calculations [24, 25] with central NN and ΛN potentials, reproducing $B_\Lambda = 0.13$ MeV [5] and $\langle r_\Lambda^2 \rangle^{1/2} = 11.2$ fm for $d + \Lambda$ in ${}^3_\Lambda\text{H}$ ($J^P = 1/2^+$, g.s.). We use $\varphi_0^{(N)}$ obtained in three-

body NNN calculations [26], and $C_{TS}^2 = 3/2$ in Eq. (5). Figure 1 shows the relative density distributions $\rho_\Lambda(r) = |\varphi_0^{(\Lambda)}(r)|^2$ for Λ in ${}^3,4\text{H}_{g.s.}$, as a function of the relative distance between the core nucleus and Λ , together with relative density distributions $\rho_N(r) = |\varphi_0^{(N)}(r)|^2$ for N in ${}^3,4\text{He}$. We confirm that the Λ density distribution for ${}^4\text{H}_{g.s.}$ is significantly suppressed at the nuclear center and is pushed outside [11, 27], and that the Λ density distribution for ${}^3\text{H}_{g.s.}$ indicates the weakly bound state having a long tail.

Considering the spin-flip $\Delta S = 1$ production in the ${}^4\text{He}(K^-, \pi^0)$ reaction, we obtain the production cross section of an unnatural-parity state of ${}^4\text{H}(J^P = 1^+, \text{exc})$. Due to such a s -shell hypernuclear state, the differential cross section is also written by the effective number of nucleons $Z_{\text{eff}}^{J^P}$ with $\alpha \langle d\sigma/d\Omega \rangle_{\text{lab}}^{\text{elem}} = \alpha |\bar{g}_{\pi^0\Lambda}|^2$ for the in-medium $K^-p \rightarrow \pi^0\Lambda$ $\Delta S = 1$ reaction, as given in Eq. (4). We use $\varphi_0^{(\Lambda)}$ obtained by the $3N$ - Λ model with central ΛN potentials for $J^P = 1^+$, reproducing $B_\Lambda = 1.09$ MeV with respect to the ${}^3\text{H}$ - Λ threshold [10] with $\langle r_\Lambda^2 \rangle^{1/2} = 4.60$ fm, and $C_{TS}^2 = 1$ in Eq. (5).

C. ${}^3\text{H}(J^P = 3/2^+, \text{exc})$ as a virtual state

We have no observation of a $J^P = 3/2^+$ excited state of ${}^3\text{H}$ experimentally so far. It seems that there is no bound state in $J^P = 3/2^+$, but this state would be in the continuum region above the d - Λ threshold [18] as a resonant state or a virtual state theoretically. If a pole of the S matrix for a virtual state is sufficiently close to the physical axis on the complex momentum plane, it may provide an appreciable influence on the cross section at low energy [28]. This phenomenon is regarded as *threshold effects* caused by a virtual state close to the threshold. To see this situation, we study the s -wave $3/2^+$ state in ${}^3\text{H}$ with a folding model d - Λ potential $U_{\Lambda d}$, adjusting to the Λd scattering length of $a_{3/2}^{\Lambda d} = -16.2$ fm and the effective range of $r_{3/2}^{\Lambda d} = 3.2$ fm [12] for the NSC97f potential. Numerically solving the Lippmann-Schwinger equation for this $d + \Lambda$ system, we find that its pole of the S matrix is located at $k_{\Lambda d}^{(\text{pole})} = -0.057i$ fm $^{-1}$ on the complex momentum plane, which corresponds to $E_{\Lambda d}^{(\text{pole})} = -0.089$ MeV on the unphysical sheet $[-]$ of the complex E plane [29]. This state is identified as a virtual state close to the d - Λ threshold, as recently discussed by Schäfer et al. [12]. To describe the virtual state of ${}^3\text{H}(J^P = 3/2^+, \text{exc})$, we construct a continuum-discretized wave function $\hat{\varphi}_0^{(\Lambda)}$, which is given by an appropriate momentum bin of k_0 and

k_1 [30]:

$$\hat{\phi}_0^{(\Lambda)}(\mathbf{r}) = \frac{1}{\sqrt{\Delta k}} \int_{k_0}^{k_1} \phi_0^{d+\Lambda}(k, \mathbf{r}) dk, \quad (8)$$

where $\Delta k = k_1 - k_0$, and \mathbf{r} and k are the radial coordinate and the relative momentum between d and Λ , respectively, and $\phi_0^{d+\Lambda}(k, \mathbf{r})$ is a $d + \Lambda$ scattering wave function with the energy $\varepsilon_{\Lambda d} = k^2/(2\mu_{\Lambda d})$ (> 0), where $\mu_{\Lambda d}$ is the reduced mass of the $d + \Lambda$ system. This continuum-discretized wave function $\hat{\phi}_0^{(\Lambda)}$ satisfies the *positive* energy $\hat{\varepsilon}_{\Lambda d} = \{(k_1 + k_0)^2/4 + (\Delta k)^2/12\}/(2\mu_{\Lambda d})$ [30]. When we choose the momentum bin of $k_0 = 0.026 \text{ fm}^{-1}$ and $k_1 = 0.083 \text{ fm}^{-1}$ for ${}^3_{\Lambda}\text{H}$ ($J^P = 3/2^+$, exc), we find that the wave functions of $\phi_0^{d+\Lambda}(k, \mathbf{r})$ in Eq. (8) significantly enhance at the nuclear interior due to the threshold effects caused by the virtual state [31]. Thus, the continuum-discretized wave function $\hat{\phi}_0^{(\Lambda)}$ labeled by $\hat{\varepsilon}_{\Lambda d} = 0.089 \text{ MeV}$ provides an appropriate description of these threshold effects, consistent with the virtual-state phenomenon having a peak around $\hat{\varepsilon}_{\Lambda d} \simeq |E_{\Lambda d}^{(\text{pole})}|$ above the threshold in the nuclear response function [32]. Regarding $\hat{\phi}_0^{(\Lambda)}$ as $\varphi_0^{(\Lambda)}$ in Eq. (7), therefore, we can estimate the production cross sections of ${}^3_{\Lambda}\text{H}$ ($J^P = 3/2^+$, exc) as the virtual state with $C_{TS}^2 = 4/3$, as given in Eq. (5). In Fig. 1, we also display the relative density distribution $\rho_{\Lambda}(r)$ for ${}^3_{\Lambda}\text{H}$ ($J^P = 3/2^+$, exc), which leads to $\langle r_{\Lambda}^2 \rangle^{1/2} = 18.2 \text{ fm}$, in comparison with ${}^3_{\Lambda}\text{H}$ ($J^P = 1/2^+$, g.s.).

III. RESULTS AND DISCUSSION

A. Optimal Fermi-averaged differential cross sections

It has been recognized that in the standard DWIA, the in-medium $K^-p \rightarrow \pi^0\Lambda$ cross section of $\alpha\langle d\sigma/d\Omega \rangle_{\text{lab}}^{\text{elem}}$ in Eq. (4) plays an important role in explaining the production cross section of $d\sigma/d\Omega_{\text{lab}}$ in the nuclear reaction. To realize a more quantitative description in our calculations, we need to obtain the in-medium $K^-p \rightarrow \pi^0\Lambda$ cross section with the optimal Fermi-averaging t matrix [13] for the nuclear (K^-, π^0) reaction, taking into account momenta arising from the distorted waves of K^- and π^0 in the nucleus.

Figure 2 displays the angular distributions of the in-medium $K^-p \rightarrow \pi^0\Lambda$ differential cross sections for non-spin-flip $\Delta S = 0$ and spin-flip $\Delta S = 1$ productions, which are denoted by $\alpha\langle d\sigma/d\Omega \rangle_{\text{lab}}^{\text{elem}} = \alpha|\bar{f}_{\pi^0\Lambda}|^2$ and $\alpha|\bar{g}_{\pi^0\Lambda}|^2$, respectively, in the (K^-, π^0) reactions on ${}^3,4\text{He}$

at $p_{K^-} = 1.0$ GeV/ c . These behaviors affect the angular distributions of the productions of ${}^3_{}{}^4_{}{}_{\Lambda}\text{H}$, as well as the behavior of Z_{eff} that depends on the angle of θ_{lab} . Note that the absolute values and shapes of $\alpha|\bar{f}_{\pi^0\Lambda}|^2$ on ${}^4\text{He}$ and ${}^3\text{He}$ differ moderately in the $\Delta S = 0$ productions. This difference stems from the nature of the energy and momentum transfers (ω , \mathbf{q}) that satisfy the on-shell energy condition in the optimal Fermi-averaging procedure

$$\begin{aligned}\omega &\simeq m_{\Lambda} - m_N + \frac{\mathbf{q}^2}{2m_{\Lambda}} + \frac{\mathbf{p}_N^* \cdot \mathbf{q}}{m_{\Lambda}} - \frac{m_{\Lambda} - m_N}{m_{\Lambda}} \frac{\mathbf{p}_N^{*2}}{2m_N} \\ &= m_{\Lambda} - m_N - B_{\Lambda} + B_N + T_{\text{recoil}},\end{aligned}\quad (9)$$

where \mathbf{p}_N^* is the momentum of a struck nucleon and T_{recoil} is the recoil energy to the final state. Because the nucleon binding energy of $B_N = 19.8$ MeV for ${}^4\text{He}$ is so larger than that of $B_N = 5.49$ MeV for ${}^3\text{He}$, the energy difference $\Delta\omega = |\omega_4 - \omega_3|$ becomes ~ 11 MeV, where ω_4 and ω_3 are the energy transfers to ${}^4_{\Lambda}\text{H}$ and ${}^3_{\Lambda}\text{H}$, respectively. This value is comparable to $\mathbf{q}^2/2m_{\Lambda} \simeq 3.6\text{--}12$ MeV in the near-recoilless (K^- , π^0) reactions at $\theta_{\text{lab}} = 0^\circ\text{--}8^\circ$. As a result, it induces a significant downward energy shift to the Λ production threshold in the nuclear (K^- , π^0) reactions on ${}^4\text{He}$, rather than ${}^3\text{He}$. This fact leads to the difference in $\alpha|\bar{f}_{\pi^0\Lambda}|^2$ between ${}^4\text{He}$ and ${}^3\text{He}$ owing to the energy dependence of the elementary amplitude $f_{\pi^0\Lambda}$ at the forward angles of θ_{lab} . On the other hand, we find that the values of $\alpha|\bar{g}_{\pi^0\Lambda}|^2$ in the $\Delta S = 1$ productions on ${}^4\text{He}$ and ${}^3\text{He}$ are very similar.

B. ${}^4_{\Lambda}\text{H}$ ($J = 0^+$, g.s.) and ${}^4_{\Lambda}\text{H}$ ($J^P = 1^+$, exc)

Now we estimate numerically the production cross sections of ${}^4_{\Lambda}\text{H}$ in the exothermic ${}^4\text{He}(K^-, \pi^0)$ reactions at $p_{K^-} = 1.0$ GeV/ c and $\theta_{\text{lab}} = 0^\circ\text{--}20^\circ$, where the momentum transfers become $q \simeq 90\text{--}345$ MeV/ c . In Table II, we list the calculated results of $\alpha\langle d\sigma/d\Omega \rangle_{\text{lab}}^{\text{elem}}$, Z_{eff} , and $d\sigma/d\Omega_{\text{lab}}$ for ${}^4_{\Lambda}\text{H}$ ($J = 0^+$, g.s.) and ${}^4_{\Lambda}\text{H}$ ($J^P = 1^+$, exc) in the DWIA using the distortion parameters of $(\sigma_{K^-}, \sigma_{\pi}) = (45 \text{ mb}, 32 \text{ mb})$. We obtain $d\sigma/d\Omega_{\text{lab}}(0^+_{\text{g.s.}}) = 1184.3, 552.2, 100.8,$ and $19.2 \mu\text{b/sr}$ and $d\sigma/d\Omega_{\text{lab}}(1^+_{\text{exc}}) = 0.27, 10.5, 14.4,$ and $5.68 \mu\text{b/sr}$ at $\theta_{\text{lab}} = 0^\circ, 6^\circ, 12^\circ,$ and 18° , respectively. In Fig. 3, we show the calculated angular distributions of $d\sigma/d\Omega_{\text{lab}}$ for the $0^+_{\text{g.s.}}$ and 1^+_{exc} states in ${}^4_{\Lambda}\text{H}$ via the ${}^4\text{He}(K^-, \pi^0)$ reactions at $p_{K^-} = 1.0$ GeV/ c in the DWIA. We find that the production cross section of the $0^+_{\text{g.s.}}$ state dominates in the forward angles, whereas the production of the 1^+_{exc} state is comparable to that of the $0^+_{\text{g.s.}}$ state beyond $\theta_{\text{lab}} = 20^\circ$; we have $[d\sigma/d\Omega_{\text{lab}}(0^+_{\text{g.s.}})]/[d\sigma/d\Omega_{\text{lab}}(1^+_{\text{exc}})] \simeq 2.5$ at $\theta_{\text{lab}} \simeq 20^\circ$.

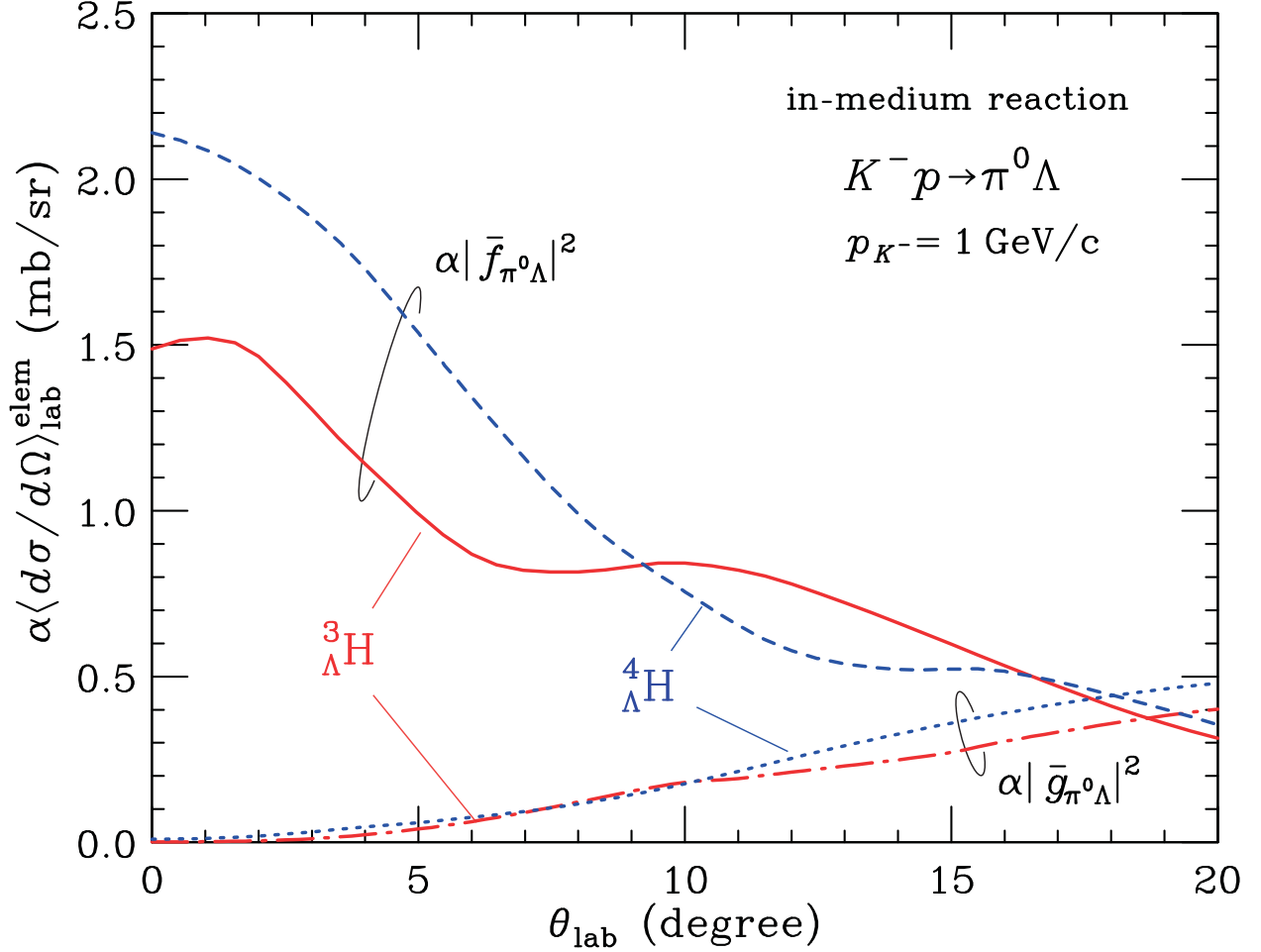


FIG. 2: Angular distributions of the in-medium $K^-p \rightarrow \pi^0\Lambda$ differential cross sections $\alpha\langle d\sigma/d\Omega \rangle_{\text{lab}}^{\text{elem}} = \alpha|\bar{f}_{\pi^0\Lambda}|^2$ for the non-spin-flip $\Delta S = 0$ production in the (K^-, π^0) reactions at $p_{K^-} = 1.0$ GeV/c, and those of $\alpha|\bar{g}_{\pi^0\Lambda}|^2$ for the spin-flip $\Delta S = 1$ production. Solid and dot-dashed (dashed and dotted) curves denote the calculated results for ${}^3_{\Lambda}\text{H}$ (${}^4_{\Lambda}\text{H}$) production on the ${}^3\text{He}$ (${}^4\text{He}$) target, respectively. The optimal Fermi-averaging $K^-p \rightarrow \pi^0\Lambda$ amplitudes of $\bar{f}_{\pi^0\Lambda}$ and $\bar{g}_{\pi^0\Lambda}$ are obtained [13] in the use of the elementary amplitudes analyzed by Gopal, et al. [20].

The integrated cross section of ${}^4_{\Lambda}\text{H}$ over $\theta_{\text{lab}} = 0^\circ\text{--}20^\circ$ is given by

$$\sigma_{\text{lab}}(J_B^P) \equiv \int_{\theta_{\text{lab}}=0^\circ}^{\theta_{\text{lab}}=20^\circ} \left(\frac{d\sigma}{d\Omega} \right)_{\text{lab}, \theta_{\text{lab}}}^{J_B^P} d\Omega. \quad (10)$$

We find $\sigma_{\text{lab}}(0_{\text{g.s.}}^+) = 63.1 \mu\text{b}$ and $\sigma_{\text{lab}}(1_{\text{exc}}^+) = 3.8 \mu\text{b}$ at $p_{K^-} = 1.0$ GeV/c in the DWIA, compared with $\sigma_{\text{lab}}(0_{\text{g.s.}}^+) = 150.4 \mu\text{b}$ and $\sigma_{\text{lab}}(1_{\text{exc}}^+) = 10.7 \mu\text{b}$ in the PWIA. This implies that distortion effects are remarkably important in quantitative estimations for the $A =$

TABLE II: Calculated angular distributions of the laboratory differential cross sections for the $0_{\text{g.s.}}^+$ and 1_{exc}^+ states in ${}^4_{\Lambda}\text{H}$ via the ${}^4\text{He}(K^-, \pi^0)$ reactions at $p_{K^-} = 1.0 \text{ GeV}/c$ in the DWIA. The distortion parameters of $(\sigma_{K^-}, \sigma_{\pi}) = (45 \text{ mb}, 32 \text{ mb})$ are used.

θ_{lab} (degree)	q (MeV/c)	${}^4_{\Lambda}\text{H} (J^P = 0^+, \text{g.s.})$			${}^4_{\Lambda}\text{H} (J^P = 1^+, \text{exc})$		
		$\alpha \langle d\sigma/d\Omega \rangle_{\text{lab}}^{\text{elem}}$ (mb/sr)	Z_{eff} ($\times 10^{-1}$)	$d\sigma/d\Omega_{\text{lab}}$ ($\mu\text{b/sr}$)	$\alpha \langle d\sigma/d\Omega \rangle_{\text{lab}}^{\text{elem}}$ (mb/sr)	Z_{eff} ($\times 10^{-1}$)	$d\sigma/d\Omega_{\text{lab}}$ ($\mu\text{b/sr}$)
0	90	2.140	5.534	1184.3	0.001	2.298	0.27
2	96	2.003	5.353	1072.3	0.004	2.218	0.98
4	113	1.729	4.848	838.1	0.023	1.996	4.55
6	135	1.342	4.116	552.2	0.062	1.678	10.5
8	162	0.990	3.283	325.1	0.122	1.321	16.1
10	191	0.756	2.465	186.3	0.181	0.977	17.7
12	221	0.578	1.745	100.8	0.212	0.680	14.4
14	251	0.521	1.165	60.8	0.249	0.446	11.1
16	282	0.516	0.733	37.8	0.305	0.275	8.38
18	314	0.445	0.433	19.2	0.358	0.159	5.68
20	345	0.355	0.237	8.42	0.402	0.085	3.42

4 nuclear systems [11]. The distortion effects are roughly estimated by a distortion factor $D_{\text{dis}} \equiv Z_{\text{eff}}^{\text{DW}}/Z_{\text{eff}}^{\text{PW}}$ in the eikonal meson waves. We find $D_{\text{dis}} \simeq 0.42\text{--}0.23$ for ${}^4_{\Lambda}\text{H}$, which depend on $\theta_{\text{lab}} = 0^\circ\text{--}20^\circ$. Consequently, we show that the production ratio of $\sigma_{\text{lab}}(1_{\text{exc}}^+)$ to $\sigma_{\text{lab}}(0_{\text{g.s.}}^+)$ amounts to

$$R_4 = \sigma_{\text{lab}}(1_{\text{exc}}^+)/\sigma_{\text{lab}}(0_{\text{g.s.}}^+) \simeq 0.06\text{--}0.07 \quad \text{for } {}^4_{\Lambda}\text{H} \quad (11)$$

at $p_{K^-} = 1.0 \text{ GeV}/c$.

C. ${}^3_{\Lambda}\text{H} (J^P = 1/2^+, \text{g.s.})$ and ${}^3_{\Lambda}\text{H} (J^P = 3/2^+, \text{exc})$

Let us estimate numerically the production cross sections of ${}^3_{\Lambda}\text{H}$ in the ${}^3\text{He}(K^-, \pi^0)$ reactions at $p_{K^-} = 1.0 \text{ GeV}/c$ and $\theta_{\text{lab}} = 0^\circ\text{--}20^\circ$, where the momentum transfers become $q \simeq 80\text{--}350 \text{ MeV}/c$. In Table III, we list the calculated results of $\alpha \langle d\sigma/d\Omega \rangle_{\text{lab}}^{\text{elem}}$, Z_{eff} , and

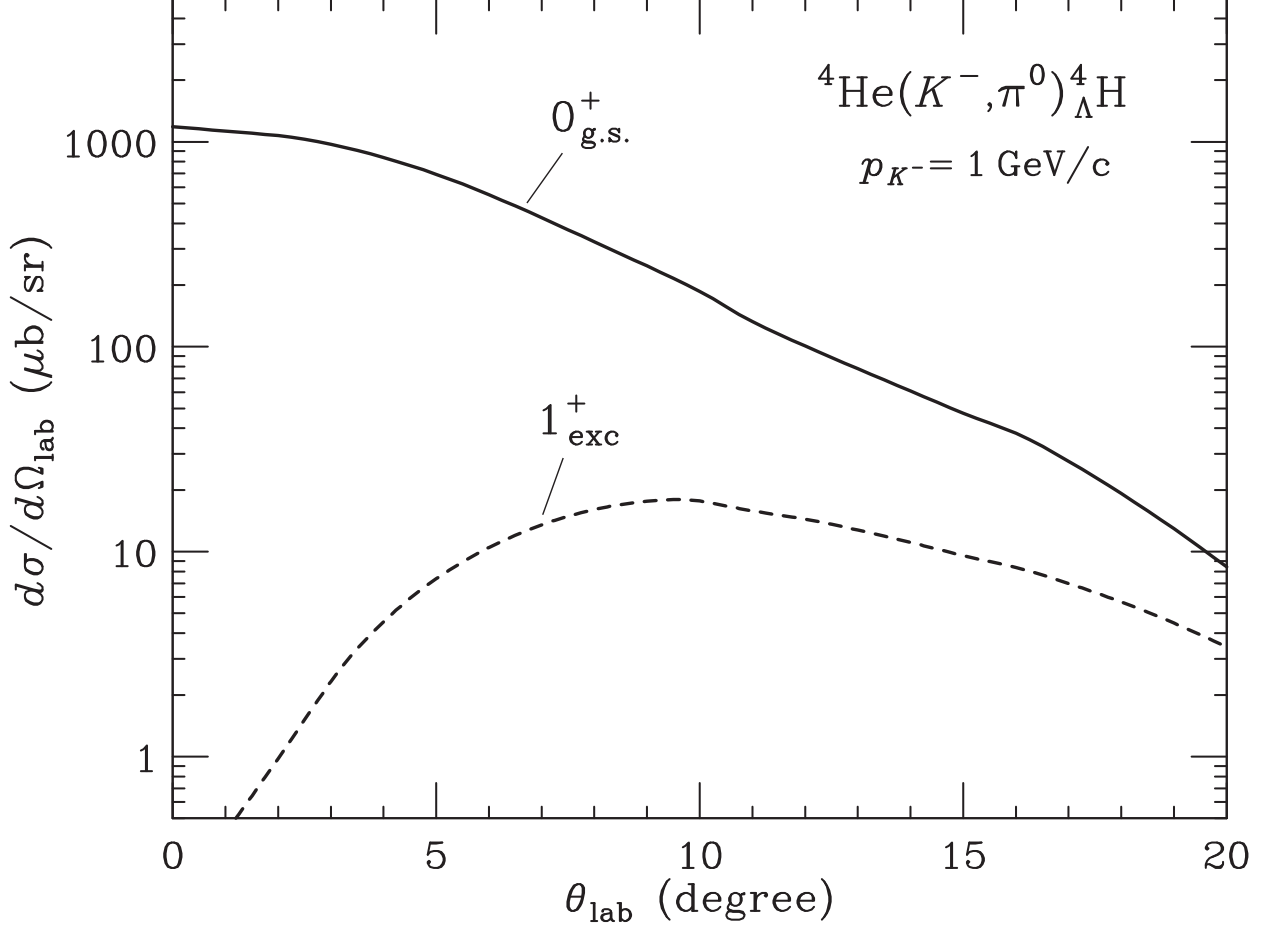


FIG. 3: Calculated angular distributions of the laboratory differential cross sections $d\sigma/d\Omega_{\text{lab}}$ for $0_{\text{g.s.}}^+$ and 1_{exc}^+ states in ${}^4_{\Lambda}\text{H}$ via the ${}^4\text{He}(K^-, \pi^0){}^4_{\Lambda}\text{H}$ reactions at $p_{K^-} = 1.0$ GeV/c in the DWIA.

$d\sigma/d\Omega_{\text{lab}}$ for ${}^3_{\Lambda}\text{H}(J^P = 1/2^+, \text{g.s.})$ and ${}^3_{\Lambda}\text{H}(J^P = 3/2^+, \text{exc})$ in the DWIA using the distortion parameters of $(\sigma_{K^-}, \sigma_{\pi}) = (45 \text{ mb}, 32 \text{ mb})$. We obtain $d\sigma/d\Omega_{\text{lab}}(1/2_{\text{g.s.}}^+) = 484.0, 183.4, 57.1, \text{ and } 7.5 \text{ } \mu\text{b/sr}$, and $d\sigma/d\Omega_{\text{lab}}(3/2_{\text{exc}}^+) = 1.67, 2.94, 2.83, \text{ and } 1.01 \text{ } \mu\text{b/sr}$ at $\theta_{\text{lab}} = 0^\circ, 6^\circ, 12^\circ, \text{ and } 18^\circ$, respectively. In Fig. 4, we show the calculated angular distributions of $d\sigma/d\Omega_{\text{lab}}$ for the $1/2_{\text{g.s.}}^+$ and $3/2_{\text{exc}}^+$ states in ${}^3_{\Lambda}\text{H}$ via the ${}^3\text{He}(K^-, \pi^0){}^3_{\Lambda}\text{H}$ reactions at $p_{K^-} = 1.0$ GeV/c in the DWIA. We find that the production cross section of $d\sigma/d\Omega_{\text{lab}}$ for the $1/2_{\text{g.s.}}^+$ state is dominant at the forward angles of $\theta_{\text{lab}} = 0^\circ\text{--}20^\circ$, in comparison with that for $3/2_{\text{exc}}^+$ state; we have $[d\sigma/d\Omega_{\text{lab}}(1/2_{\text{g.s.}}^+)]/[d\sigma/d\Omega_{\text{lab}}(3/2_{\text{exc}}^+)] \simeq 5.6$ at $\theta_{\text{lab}} \simeq 20^\circ$.

To study the feasibility of the lifetime measurements of ${}^3_{\Lambda}\text{H}$ at the J-PARC experiments, we estimate the integrated cross sections of σ_{lab} over $\theta_{\text{lab}} = 0^\circ\text{--}20^\circ$, as given in Eq. (10), in comparison with those of ${}^4_{\Lambda}\text{H}$. We find $\sigma_{\text{lab}}(1/2_{\text{g.s.}}^+) = 25.9 \text{ } \mu\text{b}$ and $\sigma_{\text{lab}}(3/2_{\text{exc}}^+) = 0.77 \text{ } \mu\text{b}$ at

$p_{K^-} = 1.0$ GeV/ c in the DWIA, compared with $\sigma_{\text{lab}}(1/2_{\text{g.s.}}^+) = 43.7$ μb and $\sigma_{\text{lab}}(3/2_{\text{exc}}^+) = 1.4$ μb in the PWIA. The distortion factor for ${}^3_{\Lambda}\text{H}$ becomes $D_{\text{dis}} \simeq 0.67\text{--}0.38$ at $\theta_{\text{lab}} = 0^\circ\text{--}20^\circ$. As a result, the production ratio of $\sigma_{\text{lab}}(3/2_{\text{exc}}^+)$ to $\sigma_{\text{lab}}(1/2_{\text{g.s.}}^+)$ amounts to

$$R_3 = \sigma_{\text{lab}}(3/2_{\text{exc}}^+)/\sigma_{\text{lab}}(1/2_{\text{g.s.}}^+) \simeq 0.030\text{--}0.033 \quad \text{for } {}^3_{\Lambda}\text{H} \quad (12)$$

at $p_{K^-} = 1.0$ GeV/ c . In comparison with $\sigma_{\text{lab}}(1_{\text{exc}}^+)$ in ${}^4_{\Lambda}\text{H}$, we realize that the reduction of $\sigma_{\text{lab}}(3/2_{\text{exc}}^+)$ in ${}^3_{\Lambda}\text{H}$ stems from a spread-out transition density $\rho_{\text{tr}}(r)$ in Eq. (7) due to $\langle r_{\Lambda}^2 \rangle^{1/2} = 18.2$ fm for the Λ wave function of the $3/2^+$ state of ${}^3_{\Lambda}\text{H}$, whereas the absolute value of $\sigma_{\text{lab}}(3/2_{\text{exc}}^+)$ depends on its pole position of the S matrix for the virtual state.

The STAR Collaboration [6] recently reported the Λ separation energy of $B_{\Lambda} = 0.41 \pm 0.12$ MeV for the $1/2_{\text{g.s.}}^+$ state of ${}^3_{\Lambda}\text{H}$. To see the effects of the Λ separation energy on the Λ production, we estimate the production cross section of ${}^3_{\Lambda}\text{H}$ in the (K^-, π^0) reaction at $p_{K^-} = 1.0$ GeV/ c , reproducing $B_{\Lambda} = 0.41$ MeV by an additional attraction in the ΛN interaction. We find that the integrated cross section in the DWIA amounts to $\sigma_{\text{lab}}(1/2_{\text{g.s.}}^+) = 41.0$ μb , which is 60% larger than $\sigma_{\text{lab}}(1/2_{\text{g.s.}}^+) = 25.9$ μb for $B_{\Lambda} = 0.13$ MeV. This is because the transition density $\rho_{\text{tr}}(r)$ in Eq. (7) becomes large, where the Λ wave function of $\varphi_0^{(\Lambda)}(r)$ is shifted into the nuclear inside due to the additional attraction, leading to $\langle r_{\Lambda}^2 \rangle^{1/2} = 6.81$ fm. Therefore, we suggest that a precise measurement of the production cross section of ${}^3_{\Lambda}\text{H}$ gives valuable information concerning the value of B_{Λ} with studying the nature of the ΛN interaction and the structure of ${}^3_{\Lambda}\text{H}$.

D. Recoil effects

We have recognized that the recoil effects are essential in production reactions on the very light nuclear target such as ${}^4\text{He}$ [11]. Thus, the recoil correction may significantly enlarge the production cross sections because the *effective* momentum transfers denote $q_{\text{eff}} \simeq 51\text{--}223$ MeV/ c at $\theta_{\text{lab}} = 0^\circ\text{--}20^\circ$ with $M_C/M_D = 0.647$ for ${}^3_{\Lambda}\text{H}$, which achieve the Λ production in the near-recoilless reaction, rather than $q_{\text{eff}} \simeq 66\text{--}253$ MeV/ c with $M_C/M_D = 0.734$ for ${}^4_{\Lambda}\text{H}$. When the recoil correction is omitted ($M_C/M_D \rightarrow 1$), the integrated cross sections amount to $\sigma_{\text{lab}}({}^3_{\Lambda}\text{H}; 1/2_{\text{g.s.}}^+) = 9.74$ μb and $\sigma_{\text{lab}}({}^4_{\Lambda}\text{H}; 0_{\text{g.s.}}^+) = 35.2$ μb in the DWIA, and $\sigma_{\text{lab}}({}^3_{\Lambda}\text{H}; 1/2_{\text{g.s.}}^+) = 17.9$ μb and $\sigma_{\text{lab}}({}^4_{\Lambda}\text{H}; 0_{\text{g.s.}}^+) = 89.9$ μb in the PWIA. The values of σ_{lab} with the recoil effects are larger than those of σ_{lab} without the recoil effects by a factor of about 2.5 (1.7) for ${}^3_{\Lambda}\text{H}$

TABLE III: Calculated angular distributions of the laboratory differential cross sections for the $1/2_{\text{g.s.}}^+$ and $3/2_{\text{exc}}^+$ states in ${}^3_{\Lambda}\text{H}$ via the ${}^3\text{He}(K^-, \pi^0)$ reactions at $p_{K^-} = 1.0$ GeV/ c in the DWIA. The distortion parameters of $(\sigma_{K^-}, \sigma_{\pi}) = (45 \text{ mb}, 32 \text{ mb})$ are used.

θ_{lab} (degree)	q (MeV/ c)	${}^3_{\Lambda}\text{H} (J^P = 1/2^+, \text{g.s.})$			${}^3_{\Lambda}\text{H} (J^P = 3/2^+, \text{exc})$		
		$\alpha \langle d\sigma/d\Omega \rangle_{\text{lab}}^{\text{elem}}$ (mb/sr)	Z_{eff} ($\times 10^{-1}$)	$d\sigma/d\Omega_{\text{lab}}$ ($\mu\text{b/sr}$)	$\alpha \langle d\sigma/d\Omega \rangle_{\text{lab}}^{\text{elem}}$ (mb/sr)	Z_{eff} ($\times 10^{-1}$)	$d\sigma/d\Omega_{\text{lab}}$ ($\mu\text{b/sr}$)
0	79	1.488	3.253	484.0	0.010	0.668	0.67
2	86	1.465	3.090	452.8	0.019	0.626	1.19
4	104	1.141	2.664	304.1	0.047	0.520	2.43
6	129	0.869	2.110	183.4	0.075	0.390	2.94
8	157	0.815	1.560	127.2	0.116	0.271	3.15
10	187	0.842	1.092	92.0	0.177	0.178	3.14
12	218	0.780	0.733	57.1	0.253	0.112	2.83
14	249	0.662	0.474	31.4	0.326	0.068	2.21
16	281	0.533	0.298	15.9	0.390	0.040	1.56
18	312	0.411	0.183	7.50	0.441	0.023	1.01
20	344	0.314	0.109	3.41	0.480	0.013	0.61

(${}^4_{\Lambda}\text{H}$). Therefore, we confirm the benefit of the use of the ${}^{3,4}\text{He}$ targets in the Λ production via the (K^-, π^0) reaction.

E. Comparison with ${}^{3,4}\text{He}(\pi^-, K^0)$ reactions

It is also interesting to discuss the production cross sections of ${}^{3,4}_{\Lambda}\text{H}$ in the endothermic (π^-, K^0) reactions on ${}^{3,4}\text{He}$ at $p_{\pi^-} = 1.05$ GeV/ c and $\theta_{\text{lab}} = 0^\circ\text{--}20^\circ$, where the high momentum transfers of $q \simeq 350\text{--}500$ MeV/ c are expected to bring benefits to the use of the ${}^{3,4}\text{He}$ targets [11, 33]. In Table IV, we list the calculated results of $\alpha \langle \bar{f}_{\pi^- p \rightarrow K^0 \Lambda} \rangle^2$, Z_{eff} , and $d\sigma/d\Omega_{\text{lab}}$ for ${}^3_{\Lambda}\text{H} (J^P = 1/2^+, \text{g.s.})$ and ${}^4_{\Lambda}\text{H} (J^P = 0^+, \text{g.s.})$ at 1.05 GeV/ c in the DWIA. We find the updated values of $d\sigma/d\Omega_{\text{lab}}({}^3_{\Lambda}\text{H}; 1/2_{\text{g.s.}}^+) = 7.28, 5.61, 2.62,$ and 0.78 $\mu\text{b/sr}$ and $d\sigma/d\Omega_{\text{lab}}({}^4_{\Lambda}\text{H}; 0_{\text{g.s.}}^+) = 18.82, 13.82, 5.50,$ and 1.10 $\mu\text{b/sr}$ at $\theta_{\text{lab}} = 0^\circ, 6^\circ, 12^\circ,$

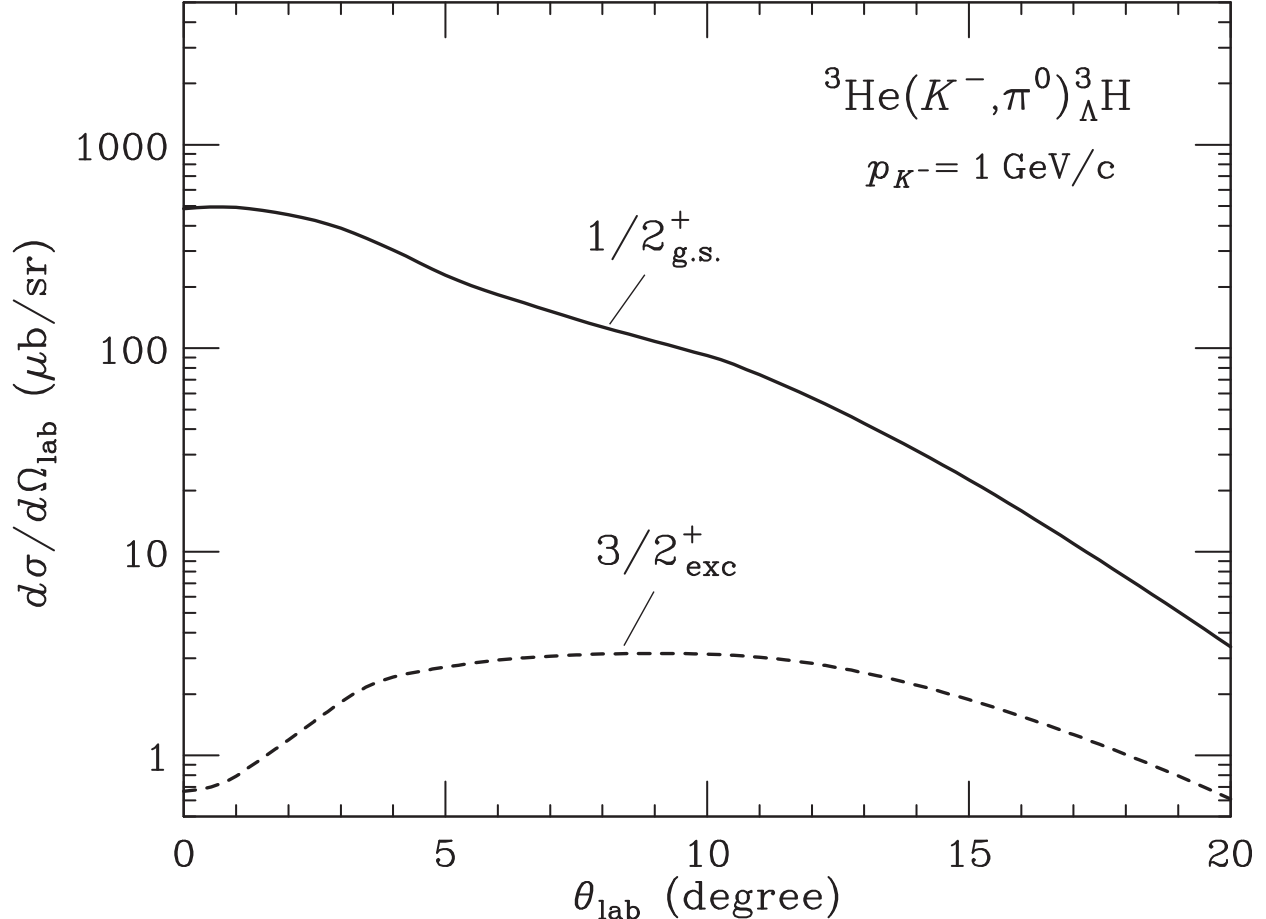


FIG. 4: Calculated angular distributions of the laboratory differential cross sections $d\sigma/d\Omega_{\text{lab}}$ for the $1/2_{\text{g.s.}}^+$ and $3/2_{\text{exc}}^+$ states in ${}^3_{\Lambda}\text{H}$ via the ${}^3\text{He}(K^-, \pi^0){}^3_{\Lambda}\text{H}$ reactions at $p_{K^-} = 1.0$ GeV/ c in the DWIA.

and 18° , respectively, compared with the previous works [11, 33]. These results lead to $\sigma_{\text{lab}}({}^3_{\Lambda}\text{H}; 1/2_{\text{g.s.}}^+) = 0.93 \mu\text{b}$ and $\sigma_{\text{lab}}({}^4_{\Lambda}\text{H}; 0_{\text{g.s.}}^+) = 2.02 \mu\text{b}$. Note that the angular dependences of $\alpha|\bar{f}_{\pi^-p \rightarrow K^0\Lambda}|^2$ for ${}^4_{\Lambda}\text{H}$ and ${}^3_{\Lambda}\text{H}$ are very similar in the (K^-, π^0) reactions at $\theta_{\text{lab}} = 0^\circ$ – 20° , whereas the absolute values of the former are slightly larger than those of the latter.

Moreover, we find that the values of $d\sigma/d\Omega_{\text{lab}}({}^3_{\Lambda}\text{H}; 1/2_{\text{g.s.}}^+)$ in the region of $q > 350$ MeV/ c are enhanced by more than 14% owing to the use of the CDCC wave functions for ${}^3_{\Lambda}\text{H}$ in our calculations, in comparison with those obtained by omitting the couplings between $[d \otimes \Lambda]$ and $[(d^*)_n \otimes \Lambda]$ channels in the CDCC, where $(d^*)_n$ denote the n -th continuum-discretized excited states of the deuteron core nucleus. This implies that the excited-state components of $(d^*)_n$ contribute to the ${}^3_{\Lambda}\text{H}$ production [25], so its production yield grows with increasing

TABLE IV: Calculated angular distributions of the laboratory differential cross sections for ${}^3_{\Lambda}\text{H}$ in the ${}^3,4\text{He}(\pi^-, K^0)$ reactions at $p_{\pi^-} = 1.05 \text{ GeV}/c$ in the DWIA. The distortion parameters of $(\sigma_{\pi}, \sigma_{K^+}) = (30 \text{ mb}, 15 \text{ mb})$ are used.

θ_{lab} (degree)	${}^3_{\Lambda}\text{H} (J^P = 1/2^+, \text{g.s.})$				${}^4_{\Lambda}\text{H} (J^P = 0^+, \text{g.s.})$			
	q (MeV/c)	$\alpha \langle d\sigma/d\Omega \rangle_{\text{lab}}^{\text{elem}}$ ($\mu\text{b}/\text{sr}$)	Z_{eff} ($\times 10^{-2}$)	$d\sigma/d\Omega_{\text{lab}}$ ($\mu\text{b}/\text{sr}$)	q (MeV/c)	$\alpha \langle d\sigma/d\Omega \rangle_{\text{lab}}^{\text{elem}}$ ($\mu\text{b}/\text{sr}$)	Z_{eff} ($\times 10^{-2}$)	$d\sigma/d\Omega_{\text{lab}}$ ($\mu\text{b}/\text{sr}$)
0	351	570.7	1.276	7.28	362	624.0	3.015	18.82
2	352	567.2	1.247	7.07	364	618.7	2.938	18.18
4	357	556.7	1.164	6.48	368	603.3	2.719	16.40
6	364	539.4	1.040	5.61	375	579.0	2.387	13.82
8	374	515.7	0.890	4.59	384	547.7	1.988	10.89
10	386	486.3	0.732	3.56	395	511.0	1.568	8.01
12	400	452.0	0.579	2.62	408	470.7	1.168	5.50
14	416	413.9	0.443	1.83	423	428.2	0.819	3.51
16	434	373.5	0.327	1.22	440	384.6	0.536	2.06
18	453	332.3	0.234	0.78	458	341.1	0.324	1.10
20	473	291.7	0.163	0.47	477	298.7	0.176	0.53

q .

F. ${}^3_{\Lambda}\text{H}$ v.s. ${}^4_{\Lambda}\text{H}$

To compare the production cross sections between ${}^3_{\Lambda}\text{H}$ and ${}^4_{\Lambda}\text{H}$, we consider the ratio of ${}^3_{\Lambda}\text{H}$ to ${}^4_{\Lambda}\text{H}$ on the angular distributions of $d\sigma/d\Omega_{\text{lab}}$,

$$\hat{R}(\theta_{\text{lab}}) = [d\sigma/d\Omega_{\text{lab}}({}^3_{\Lambda}\text{H})]/[d\sigma/d\Omega_{\text{lab}}({}^4_{\Lambda}\text{H})]. \quad (13)$$

Here we use only the production cross sections of the ${}^3,4_{\Lambda}\text{H}$ ground states because the contributions of the ${}^3,4_{\Lambda}\text{H}$ excited states to the Λ productions are very small, as discussed above. In Fig. 5, we show the calculated values of $\hat{R}(\theta_{\text{lab}})$ in the (K^-, π^0) reaction at $1.0 \text{ GeV}/c$, together with those of $\hat{R}(\theta_{\text{lab}})$ in the (π^-, K^0) reaction at $1.05 \text{ GeV}/c$. In the (K^-, π^0)

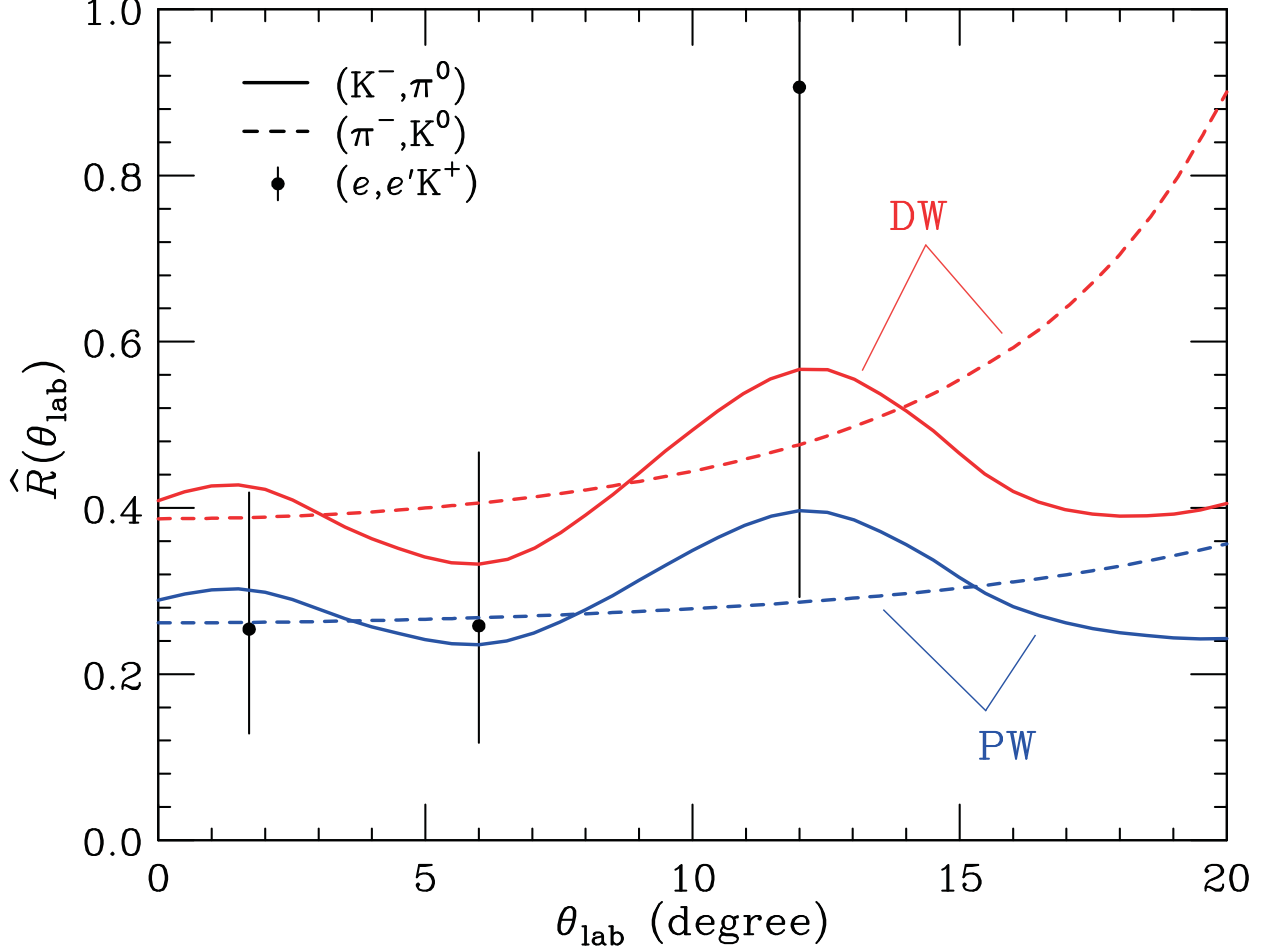


FIG. 5: Comparison among the ratios of $\hat{R}(\theta_{\text{lab}}) = [d\sigma/d\Omega_{\text{lab}}({}^3_{\Lambda}\text{H})]/[d\sigma/d\Omega_{\text{lab}}({}^4_{\Lambda}\text{H})]$ in the DW and the PW, as a function of θ_{lab} . Solid and dashed curves denote the calculated values in the (K^-, π^0) reaction at 1.0 GeV/c and the (π^-, K^0) reaction at 1.05 GeV/c, respectively. The experimental data in the $(e, e'K^+)$ reaction at the virtual photon γ^* mass $Q^2 = 3.5 \text{ GeV}^2$ are taken from Ref. [34].

reaction at 1.0 GeV/c, we find that the values of $\hat{R}(\theta_{\text{lab}})$ fluctuate in the range of 0.3–0.6 at $\theta_{\text{lab}} = 0^\circ\text{--}20^\circ$. This behavior mainly indicates the difference in $\alpha\langle d\sigma/d\Omega \rangle_{\text{lab}}^{\text{elem}}$ between ${}^3_{\Lambda}\text{H}$ and ${}^4_{\Lambda}\text{H}$, rather than the angular dependence of Z_{eff} at $\theta_{\text{lab}} = 0^\circ\text{--}20^\circ$ that correspond to $q \simeq 80\text{--}350 \text{ MeV}/c$. On the other hand, in the (π^-, K^0) reaction at 1.05 GeV/c, we find $\hat{R}(\theta_{\text{lab}}) \simeq 0.4\text{--}0.8$ at $\theta_{\text{lab}} = 0^\circ\text{--}20^\circ$ that correspond to $q \simeq 350\text{--}470 \text{ MeV}/c$. This behavior indicates the angular dependence of $Z_{\text{eff}}({}^3_{\Lambda}\text{H}_{\text{g.s.}})/Z_{\text{eff}}({}^4_{\Lambda}\text{H}_{\text{g.s.}})$, which is related to the $A = 3, 4$ form factors $F(q)$ over the Λ production processes because the angular dependences of

$\alpha\langle d\sigma/d\Omega\rangle_{\text{lab}}^{\text{elem}}$ for ${}^3_{\Lambda}\text{H}$ and ${}^4_{\Lambda}\text{H}$ are very similar. In Fig. 5, we also draw the experimental data taken from the ${}^3,4\text{He}(e, e'K^+)$ reaction at the virtual photon γ^* mass $Q^2 = 3.5 \text{ GeV}^2$ [18, 34]. It seems that the calculated results of $\hat{R}(\theta_{\text{lab}})$ in the (π^-, K^0) reaction can simulate the data of the $(e, e'K^+)$ reaction because the values of q for the former and the latter are roughly the same. Moreover, we estimate the ratio of $\sigma_{\text{lab}}({}^3_{\Lambda}\text{H})$ to $\sigma_{\text{lab}}({}^4_{\Lambda}\text{H})$ on the integrated cross sections over $\theta_{\text{lab}} = 0^\circ\text{--}20^\circ$, which is given by

$$R_{34} = \sigma_{\text{lab}}({}^3_{\Lambda}\text{H})/\sigma_{\text{lab}}({}^4_{\Lambda}\text{H}). \quad (14)$$

In the (K^-, π^0) reaction at $1.0 \text{ GeV}/c$, we find $R_{34} = 0.41$ in the DWIA. Considering some ambiguities in our eikonal-DWIA calculations, we also find $R_{34} = 0.29$ in the PWIA, omitting the distortions. Consequently, we have $R_{34} \simeq 0.3\text{--}0.4$. Note that the value of R_{34} depends on B_{Λ} for ${}^3_{\Lambda}\text{H}$; we find $R_{34} \simeq 0.65$ when we use $B_{\Lambda} = 0.41 \text{ MeV}$, as discussed in Sect. III C. It strongly suggests that the production of ${}^3_{\Lambda}\text{H}$ is a promising subject to be observed experimentally based on a successive measurement of ${}^4_{\Lambda}\text{H}$ at the J-PARC experiment. In the (π^-, K^0) reaction at $1.05 \text{ GeV}/c$, we find $R_{34} = 0.46$ in the DWIA and $R_{34} = 0.28$ in the PWIA, leading to $R_{34} \simeq 0.3\text{--}0.4$. The comparison between the nuclear (K^-, π^0) and (π^-, K^0) reactions on $\hat{R}(\theta_{\text{lab}})$ provides a better understanding of not only the structure of the ${}^3,4_{\Lambda}\text{H}$ bound states but also the production mechanism of these states.

IV. SUMMARY AND CONCLUSION

We have investigated theoretically productions of ${}^3,4_{\Lambda}\text{H}$ bound states via ${}^3,4\text{He}(K^-, \pi^0)$ reactions in the DWIA with the optimal Fermi-averaging $K^-p \rightarrow \pi^0\Lambda t$ matrix. We have calculated the laboratory differential cross sections of $d\sigma/d\Omega_{\text{lab}}$ and the integrated cross sections of σ_{lab} by the non-spin-flip $\Delta S = 0$ production in the ${}^3,4\text{He}(K^-, \pi^0)$ reactions at $1.0 \text{ GeV}/c$ and $\theta_{\text{lab}} = 0^\circ\text{--}20^\circ$, together with those by the spin-flip $\Delta S = 1$ production. We have also compared these cross sections with those in the (π^-, K^0) reactions at $1.05 \text{ GeV}/c$. The results are summarized as follows:

- (i) The calculated integrated cross sections of the $0_{\text{g.s.}}^+$ and 1_{exc}^+ states of ${}^4_{\Lambda}\text{H}$ amount to $\sigma_{\text{lab}}(0_{\text{g.s.}}^+) = 63.1 \mu\text{b}$ and $\sigma_{\text{lab}}(1_{\text{exc}}^+) = 3.8 \mu\text{b}$, respectively, leading to $R_4 = \sigma_{\text{lab}}(1_{\text{exc}}^+)/\sigma_{\text{lab}}(0_{\text{g.s.}}^+) \simeq 0.06\text{--}0.07$. The production of the $0_{\text{g.s.}}^+$ state dominates in the forward angles of $\theta_{\text{lab}} = 0^\circ\text{--}20^\circ$, in comparison with that of the $1_{\text{g.s.}}^+$ state.

- (ii) The calculated integrated cross sections of the $1/2_{\text{g.s.}}^+$ and $3/2_{\text{exc}}^+$ states of ${}^3_{\Lambda}\text{H}$ amount to $\sigma_{\text{lab}}(1/2_{\text{g.s.}}^+) = 25.9 \mu\text{b}$ and $\sigma_{\text{lab}}(3/2_{\text{exc}}^+) = 0.77 \mu\text{b}$, respectively. This leads to $R_3 = \sigma_{\text{lab}}(3/2_{\text{exc}}^+)/\sigma_{\text{lab}}(1/2_{\text{g.s.}}^+) \simeq 0.03$, of which value is a half as large as that of R_4 .
- (iii) The calculated angular distributions of the in-medium $K^-p \rightarrow \pi^0\Lambda$ differential cross sections $\alpha|\overline{f}_{\pi^0\Lambda}|^2$ for ${}^3_{\Lambda}\text{H}$ are remarkably different from those for ${}^4_{\Lambda}\text{H}$, caused by the optimal Fermi-averaging in the nuclear (K^- , π^0) reactions, whereas $\alpha|\overline{g}_{\pi^0\Lambda}|^2$ for ${}^3,4_{\Lambda}\text{H}$ are very similar to each other.
- (iv) The recoil effects are important in productions of ${}^3,4_{\Lambda}\text{H}$ owing to the benefit of the use of the ${}^3,4\text{He}$ targets via the nuclear (K^- , π^0) reactions, as well as the nuclear (π^- , K^0) reactions.

In conclusion, we show that the comparison in $d\sigma/d\Omega_{\text{lab}}$ and σ_{lab} between ${}^4_{\Lambda}\text{H}$ and ${}^3_{\Lambda}\text{H}$ provides examining the mechanism of the production and structure of ${}^3,4_{\Lambda}\text{H}$ in the (K^- , π^0) reactions on ${}^3,4\text{He}$ at $p_{K^-} = 1.0 \text{ GeV}/c$; the calculated results indicate $R_{34} = \sigma_{\text{lab}}({}^3_{\Lambda}\text{H})/\sigma_{\text{lab}}({}^4_{\Lambda}\text{H}) \simeq 0.3\text{--}0.4$. This investigation confirms the feasibility of the lifetime measurements of ${}^3_{\Lambda}\text{H}$ at the J-PARC experiments.

Acknowledgments

The authors thank Dr. Y. Ma and Dr. F. Sakuma for many valuable discussions. This work was supported by Grants-in-Aid for Scientific Research (KAKENHI) from the Japan Society for the Promotion of Science: Scientific Research (C) (Grant No. JP20K03954).

Appendix A: Explicit forms of the differential cross sections

To consider the laboratory differential cross sections of the $A(K^-, \pi)B$ reaction in the DWIA, we will define wave functions of the initial and final states, Ψ_A and Ψ_B , in the jj coupling scheme:

$$|\Psi_A\rangle = \hat{\mathcal{A}} \left[\Phi_{J_C} \otimes \phi_{(\ell_1 \frac{1}{2})j_1}^{(N)} \right]_{J_A}^{M_A}, \quad (\text{A1})$$

$$|\Psi_B\rangle = \sum_{J_C j_2} \left[\Phi_{J_C} \otimes \phi_{(\ell_2 \frac{1}{2})j_2}^{(\Lambda)} \right]_{J_B}^{M_B}, \quad (\text{A2})$$

where Φ_{J_C} , $\phi_{(\ell_1 \frac{1}{2}) j_1}^{(N)}$, and $\phi_{(\ell_2 \frac{1}{2}) j_2}^{(\Lambda)}$ are wave functions of a core nucleus, a nucleon in the target nucleus A , and Λ in the hypernucleus B , respectively. \hat{A} is the antisymmetrized operator for nucleons. The meson distorted waves for outgoing π and incoming K^- are written by the partial wave expansion

$$\chi_{\pi}^{(-)*}(\mathbf{p}_{\pi}, \mathbf{r}) \chi_{K^-}^{(+)}(\mathbf{p}_{K^-}, \mathbf{r}) = \sum_{\ell m} \sqrt{4\pi[\ell]} i^{\ell} \tilde{j}_{\ell m}(\theta_{\text{lab}}, r) Y_{\ell m}(\hat{\mathbf{r}}), \quad (\text{A3})$$

where $\tilde{j}_{\ell m}(\theta_{\text{lab}}, r)$ is the radial distorted wave with the angular momentum with (ℓ, m) , and θ_{lab} is the scattering angle to the forward direction in the nuclear (K^- , π) reaction.

The explicit form of the differential cross section with the non-spin-flip $\Delta S = 0$ processes in Eq. (1) is written as

$$\begin{aligned} \left(\frac{d\sigma}{d\Omega} \right)_{\text{lab}}^{J_B^P(\Delta S=0)} &= \alpha \sum_{\ell m c c'} (S_c^{1/2})^* (S_{c'}^{1/2}) \bar{f}_{\pi\Lambda}^* \bar{f}_{\pi\Lambda} (-)^{2J_B + J_C + J_C' - 1} \\ &\times [J_B][\ell] \sqrt{[J_C][j_2][j_1][J_C'][j_2'][j_1']} [I_{j_2 j_1 \ell}^m(\theta_{\text{lab}})]^* [I_{j_2' j_1' \ell}^m(\theta_{\text{lab}})] \\ &\times \begin{pmatrix} j_2 & \ell & j_1 \\ -\frac{1}{2} & 0 & \frac{1}{2} \end{pmatrix} \begin{Bmatrix} J_B & J_A & \ell \\ j_1 & j_2 & J_C \end{Bmatrix} \frac{[1 + (-)^{\ell_2 + \ell_1 + \ell}]}{2} \\ &\times \begin{pmatrix} j_2 & \ell & j_1 \\ -\frac{1}{2} & 0 & \frac{1}{2} \end{pmatrix} \begin{Bmatrix} J_B & J_A & \ell \\ j_1' & j_2' & J_C' \end{Bmatrix} \frac{[1 + (-)^{\ell_2' + \ell_1' + \ell}]}{2} \end{aligned} \quad (\text{A4})$$

with the integral

$$I_{j_2 j_1 \ell}^m(\theta_{\text{lab}}) = \int_0^{\infty} dr r^2 \varphi_{j_2}^{(\Lambda)*}(r) \tilde{j}_{\ell m}(\theta_{\text{lab}}, \frac{M_C}{M_D} r) \varphi_{j_1}^{(N)}(r), \quad (\text{A5})$$

where $S_c^{1/2}$ is the spectroscopic amplitude for channel $c = \{J_C j_1 j_2 \ell_1 \ell_2\}$ that may involve generally the isospin states, and the kinematical factor α arising from a translation from a two-body meson-nucleon laboratory system to a meson-nucleus laboratory system [17] is given by

$$\alpha = \frac{p_{\pi} E_{\pi}}{p_{\pi}^{(0)} E_{\pi}^{(0)}} \left(1 + \frac{E_{\pi}^{(0)} p_{\pi}^{(0)} - p_K^{(0)} \cos \theta_{\text{lab}}}{E_B^{(0)} p_{\pi}^{(0)}} \right) \left(1 + \frac{E_{\pi} p_{\pi} - p_K \cos \theta_{\text{lab}}}{E_B p_{\pi}} \right)^{-1}, \quad (\text{A6})$$

where $p_K^{(0)}$ and $p_{\pi}^{(0)}$ ($E_{\pi}^{(0)}$ and $E_B^{(0)}$) are laboratory momenta of K^- and π (laboratory energies of π and Λ) in the two-body $K^- N \rightarrow \pi \Lambda$ reaction, respectively.

For the spin-flip $\Delta S = 1$ processes, substituting the relation

$$Y_{\ell m} \boldsymbol{\sigma} \cdot \hat{\mathbf{n}} = Y_{\ell m} \sigma_y = \frac{i}{\sqrt{2}} \sum_{\mu=-1}^1 \sum_J \langle \ell m 1 \mu | J M \rangle [Y_{\ell} \otimes \sigma_1]_J^M \quad (\text{A7})$$

into Eq. (1) and using the Racah algebra, we have the differential cross section with $\Delta S = 1$, which is written by

$$\begin{aligned}
\left(\frac{d\sigma}{d\Omega}\right)_{\text{lab}}^{J_B^P(\Delta S=1)} &= \alpha \sum_{JMcc'} \sum_{\ell m \ell' m'} \sum_{\mu \mu'} (S_c^{1/2})^* (S_{c'}^{1/2}) \bar{g}_{\pi\Lambda}^* \bar{g}_{\pi\Lambda} \\
&\times \frac{1}{2} \langle \ell m 1 \mu | JM \rangle \langle JM | \ell' m' 1 \mu' \rangle (-)^{2J_B+J_C+J'_C+2J+j_1+j'_1+\ell_2+\ell'_2} \\
&\times 6 [J_B][\ell][\ell'] \sqrt{[J_C][j_2][j_1][\ell_2][\ell_1][J'_C][j'_2][j'_1][\ell'_2][\ell'_1]} \\
&\times [I_{j_2 j_1 \ell}^m(\theta_{\text{lab}})]^* [I_{j'_2 j'_1 \ell'}^m(\theta_{\text{lab}})] \\
&\times \left\{ \begin{matrix} J_B & J_A & J \\ j_1 & j_2 & J_C \end{matrix} \right\} \begin{pmatrix} \ell_2 & \ell & \ell_1 \\ 0 & 0 & 0 \end{pmatrix} \left\{ \begin{matrix} \ell_2 & \frac{1}{2} & j_2 \\ \ell_1 & \frac{1}{2} & j_1 \\ \ell & 1 & J \end{matrix} \right\} \\
&\times \left\{ \begin{matrix} J_B & J_A & J \\ j'_1 & j'_2 & J'_C \end{matrix} \right\} \begin{pmatrix} \ell'_2 & \ell' & \ell'_1 \\ 0 & 0 & 0 \end{pmatrix} \left\{ \begin{matrix} \ell'_2 & \frac{1}{2} & j'_2 \\ \ell'_1 & \frac{1}{2} & j'_1 \\ \ell' & 1 & J \end{matrix} \right\}. \tag{A8}
\end{aligned}$$

-
- [1] H. Asano, et al., ${}^3_{\Lambda}\text{H}$ and ${}^4_{\Lambda}\text{H}$ mesonic weak decay lifetime measurement with ${}^{3,4}\text{He}(K^-, \pi^0){}^3,4_{\Lambda}\text{H}$ reaction, Proposal for Nuclear and Particle Physics experiments at the J-PARC (2018); http://j-parc.jp/NuclPart/Proposal_e.html.
 - [2] M. Agnello, et al., Direct measurement of the ${}^3_{\Lambda}\text{H}$ and ${}^4_{\Lambda}\text{H}$ lifetimes using the ${}^{3,4}\text{He}(\pi^-, K^0){}^3,4_{\Lambda}\text{H}$ reactions, Proposal for Nuclear and Particle Physics experiments at the J-PARC (2019); http://j-parc.jp/NuclPart/Proposal_e.html.
 - [3] C. Rappold, et al., HypHI Collaboration, Nucl. Phys. A 913 (2013) 170.
 - [4] A. Gal, H. Garcilazo, Phys. Lett. B 791 (2019) 48 and references therein.
 - [5] M. Jurić, et al., Nucl. Phys. B 52 (1973) 1.
 - [6] J. Adam, et al., STAR Collaboration, Nature Phys. 16 (2020) 409.
 - [7] T. Harada, Phys. Rev. Lett. 81 (1998) 5287; Nucl. Phys. A 672 (2000) 181.
 - [8] T. Harada, Y. Hirabayashi, Phys. Lett. B 740 (2015) 312.
 - [9] T. Nagae, et al., Phys. Rev. Lett. 80 (1998) 1605.
 - [10] T. O. Yamamoto, et al., J-PARC E13 Collaboration, Phys. Rev. Lett. 115 (2015) 222501.
 - [11] T. Harada, Y. Hirabayashi, Phys. Rev. C 100 (2019) 024605.

- [12] M. Schäfer, B. Bazak, N. Barnea, J. Mareš, Phys. Lett. B 808 (2020) 135614.
- [13] T. Harada, Y. Hirabayashi, Nucl. Phys. A 759 (2005) 143; 767 (2006) 206.
- [14] J. Hüfner, S. Y. Lee, H. A. Weidenmüller, Nucl. Phys. A 234 (1974) 429.
- [15] C.B. Dover, L. Ludeking, G. E. Walker, Phys. Rev. C 22 (1980) 2073.
- [16] E. H. Auerbach, A. J. Baltz, C. B. Dover, A. Gal, S. H. Kahana, L. Ludeking, D. J. Millener, Ann. Phys. (N.Y.) 148 (1983) 381.
- [17] C. B. Dover, A. Gal, Ann. Phys. (N.Y.) 146 (1983) 309.
- [18] T. Mart, et al., Nucl. Phys. A 640 (1998) 235; T. Mart, B. I. S. van der Ventel, Phys. Rev. C 78 (2008) 014004.
- [19] T. Harada, Y. Hirabayashi, Phys. Rev. C 89 (2014) 054603.
- [20] G. P. Gopal, et al., Nucl. Phys. B 119 (1977) 362.
- [21] Y. Akaishi, *International Review of Nuclear Physics* 4 (World Scientific, Singapore, 1986), p. 259 and references therein.
- [22] M. Bedjidian, et al., Phys. Lett. B 62, 467 (1976); Phys. Lett. B 83, 252 (1979).
- [23] F. Schulz, et al., A1 Collaboration, Nucl. Phys. A 954 (2016) 149.
- [24] M. Kamimura, M. Yahiro, Y. Iseri, Y. Sakuragi, H. Kameyama, M. Kawai, Prog. Theor. Phys. Suppl. 89 (1986) 1.
- [25] T. Harada, Y. Hirabayashi, Nucl. Phys. A 934 (2015) 8.
- [26] Y. H. Koike, T. Harada, Nucl. Phys. A 611 (1996) 461.
- [27] Y. Kurihara, Y. Akaishi, H. Tanaka, Phys. Rev. C 31 (1985) 971.
- [28] J. R. Taylor, *Scattering Theory* (Dover, New York, 2006) p. 246.
- [29] T. Harada, Y. Hirabayashi, in *Proceedings of the 12th International Conference on Hypernuclear and Strange Particle Physics (HYP2015)*, edited by H. Tamura, et al., JPS Conf. Proc. 17 (2017) 012008.
- [30] M. Kawai, Prog. Theor. Phys. Suppl. 89 (1986) 11.
- [31] K. W. McVoy, Nucl. Phys. A 115 (1968) 481.
- [32] O. Morimatsu, K. Yazaki, Prog. Part. Nucl. Phys. 33 (1994) 679.
- [33] T. Harada, Y. Hirabayashi, in *Proceedings of 8th International Conference on Quarks and Nuclear Physics (QNP2018)*, edited by A. Doté, et al., JPS Conf. Proc. 26 (2019) 023004.
- [34] F. Dohrmann, et al., Phys. Rev. Lett. 93 (2004) 242501.